Metal-overlayer formation on C_{60} for Ti, Cr, Au, La, and In: Dependence on metal-C_{60} bonding

T. R. Ohno,* Y. Chen, S. E. Harvey, G. H. Kroll, P. J. Benning, and J. H. Weaver
Department of Materials Science and Chemical Engineering, University of Minnesota, Minneapolis, Minnesota 55455

L. P. F. Chibante and R. E. Smalley
Rice Quantum Institute and Department of Physics and Department of Chemistry, Rice University, Houston, Texas 77251
(Received 14 July 1992)

Photoelectron spectroscopy using x rays and synchrotron radiation was used to examine surface bonding and overlayer growth modes when the representative metals Ti, Cr, Au, La, and In were deposited onto thin films of pure C_{60}. None of these metals intermixed with C_{60} or formed bulk metal-fulleride compounds. Instead, metallic clusters were produced when Au, Cr, and In atoms were condensed on C_{60}. For Ti and La, the first layer formed as a monolayer but subsequent depositions produced clusters. The tendency to form a single layer for Ti and La reflects the hybridization of metal *d* and fullerene *p* orbitals, as with bulk carbides. In addition, limited amounts of metal carbide formation was evident for overlayers of Ti, La, and Cr due to some disruption of C_{60}.

INTRODUCTION

The formation of fullerene-based compounds and derivatives suggests that new forms of solid-state materials can be synthesized, possibly with important physical and chemical properties. The discovery of superconducting alkali fullerides,[1-3] for example, stimulated considerable interest. While the deposition of atoms on C_{60} can result in intercalation, as for the alkali metals, there are also several other possible behaviors. Indeed, an important question concerns what parameters determine the nature of the metal-fullerene interface. It is the study of these interfaces that is of concern here.

This paper focuses on the interaction of metal atoms and clusters with C_{60} thin films during the formation of overlayers. The purpose was to investigate metal-fullerene interface properties. Representative elements were chosen from the metal groups so as to present a range of properties such as reactivities with carbon, ionization energies, and metal cohesive energies. Titanium and chromium were chosen from the transition metals because they form carbides. Gold, a common contact metal, was chosen because it is a noble metal with no carbidic phase. Indium was chosen because of its tendency to form clusters when depositied on semiconductor surfaces. Finally, La was selected because its ionization potential is comparable to those of metals that form compounds with C_{60}, including Li, Sr, and Yb.[4-6]

EXPERIMENT

Clean surface and interface photoemission results were obtained under ultrahigh-vacuum conditions at pressures less than 1×10^{-10} Torr. In the x-ray photoemission measurements, a monochromatic Al $K\alpha$ beam ($h\nu = 1486.6$ eV) was focused to a 150-μm spot on the surface. Photoelectrons emitted at 70° relative to the surface normal were analyzed with a hemispherical analyzer and a position-sensitive resistive anode at a pass energy of 25 eV. In this spectrometer, the overall resolution of the core levels was 0.6 eV, as determined from the Fermi-level width and broadening for standard samples. Valence-band spectra were acquired using photons from Aladdin at the Wisconsin Synchrotron Radiation Center. In this case, photoelectrons were collected with an angle-integrated double-pass cylindrical mirror analyzer. The overall resolution in these valence-band studies was 0.35 eV. In both sets of experiments, ~63% of the photoemission signal came from the first layer of fullerenes, enhancing the sensitivity to changes in the surface region (the $1/e$ attenuation depth was dictated by geometric conditions).

The fullerenes were formed by the contact arc method, with subsequent separation by solution with toluene.[7] Phase-pure C_{60} was obtained by a liquid chromatography process on alumina diluted with mixtures of hexanes. The resulting C_{60} was then rinsed in methanol, dried, and placed in Ta boats that were ~6 cm from the substrates onto which C_{60} was to be condensed. Following degassing, C_{60} was evaporated by heating the boat to ~820 K. GaAs(110) surfaces were prepared by cleaving *in situ* to provide clean, flat, nonreactive substrates. For these measurements, films of ~50 Å or ~6 layers of C_{60} were condensed at room temperature.[8] Thereafter, metals were evaporated from resistively heated boats ~50 cm from the C_{60} films. After thorough outgassing, the pressure during the metal evaporation was less than 5×10^{-10} Torr. The C_{60} and metal thickness were measured with a quartz-crystal thickness monitor. The C_{60} films were maintained at room temperature during the deposition of Ti, Cr, and Au, but they were heated to 425 K during In and La deposition.

RESULTS

Au overlayers—cluster growth and bonding

Figure 1 shows representative C 1*s* energy distribution curves (EDC's) for Au deposition on C_{60}. The amount of

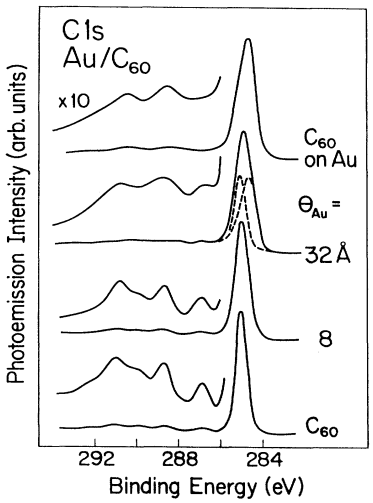

FIG. 1. Normalized C 1*s* energy distribution curves (EDC's) for Au deposition on C_{60}. The satellite features are magnified by 10 to accentuate differences observed for various coverages. The top EDC is for C_{60} chemisorbed on a polycrystalline Au substrate. This line shape is used to separate the emission for 32-Å Au deposition into a chemisorbed and bulk fullerene contribution.

Au is given alongside each EDC. The spectra are normalized to constant peak height and the satellite structures at higher binding energy are magnified to accentuate changes. The EDC at the bottom shows the C 1*s* signature of a thick C_{60} layer.[9] The main line appears at 285.0 eV and its full width at half maximum (FWHM) is 0.65 eV. The binding energy reflects the Fermi-level alignment of the fullerenes to the *n*-type GaAs substrate as a result of ~0.02 electron/molecule transfer from the semiconductor.[8] The shake-up features demonstrate the molecular character of the fullerene solid.[8] In particular, the feature at 1.9 eV higher binding energy is due to an excitation from the highest occupied molecular orbital to the lowest unoccupied molecular orbital (HOMO-LUMO) induced by the sudden creation of the core hole.[3,9] Other sharp features shifted 3–8 eV relative to the main line are due to monopole and dipole excitations superimposed on a broad plasmon at ~6.3 eV.[3,9] These observations are consistent with high-resolution electron energy loss and optical-absorption measurements.[10–12]

The deposition of Au on C_{60} results in the attenuation of the C 1*s* intensity. By ~4-Å deposition, the C 1*s* emission was slightly broadened and its intensity was reduced to ~80% of the clean layer, a smaller decrease than would be expected if a uniform layer were growing. These results indicate the formation of Au clusters. By 8-Å deposition, the C 1*s* main line broadened to 0.8-eV FWHM and the relative intensity and definition of the shake-up features were reduced, as shown in Fig. 1. Further Au deposition increased the main line width, shifted the peak maximum to lower binding energy, and made the satellites less distinct, as is evident from Fig. 1 for 32-Å Au. For all coverages the Au $4f_{7/2}$ binding energy was 83.9 eV and its line shape did not change, also indicative of cluster formation.

For clusters growing on C_{60}, there will be a contribution to the C 1*s* emission from fullerenes in contact with the Au. To isolate the line shape representative of this chemisorbed layer, we deposited submonolayer amounts of C_{60} on a thick Au film grown *in situ*. The slightly asymmetric C 1*s* main line for this case was at 284.6 eV and its FWHM was 0.9 eV, as shown at the top of Fig. 1. In addition, the C 1*s* satellites were broadened, riding on the tail of the main line. The line shape for C_{60} adsorbed on Au can be explained by the formation of a chemical bond with partial occupancy of LUMO.[8] This affects the C 1*s* line shape via changes in core-hole screening. Such an effect is commonly observed for molecules like CO that chemisorb associatively on metallic substrates.[13] The enhanced bonding of the first C_{60} layer to Au can be seen from thermal desorption of the fullerenes: multilayers could be desorbed completely at 570 K, leaving the more strongly bonded monolayer attached, as judged from the C 1*s* line shapes. The monolayer could be desorbed by heating to 620 K.

It is possible to construct the measured C 1*s* emission spectra using the line shapes for C_{60} multilayers and C_{60} molecules chemisorbed on Au. At low coverage, these constructs are not unique, but they do account for the observed broadening. At higher coverage, as for 32-Å Au, the C 1*s* main line can be separated into two components, shown by the dashed lines in Fig. 1. The morphology for this overlayer is irregular, with Au clusters dominating but also thinner Au layers through which the fullerene layer in contact with the Au could be seen with photoemission. We note that since the interaction between the metal clusters and fullerenes was stronger than C_{60}-C_{60} bonding it may lead to roughening of the starting surface.

Indium overlayers—cluster growth

Indium also forms clusters when deposited on C_{60}. Analysis of the C 1*s* and GaAs substrate emission showed that all signals decreased at the same rate, demonstrating nucleation on top of the fullerenes. In addition, the In $3d_{5/2}$ emission reflected metallic character even at 1-Å deposition, with a peak position of 443.8 eV, a slight metallic asymmetry and a plasmon loss at ~11.5 eV.[14] The deposition of 24 Å of In at ~425 K had no detectable effect on the C 1*s* line shape, indicating that the clusters were large. We found no evidence for In-C_{60} intermixing under our growth conditions, and we could see no bonding component that could be attributed to the In-C_{60} boundary layer.

Cr overlayers—cluster growth and C_{60} disruption

Vapor deposition of Cr onto C_{60} films also leads to cluster formation, as shown by analysis of the C 1*s* and GaAs substrate emission attenuation and the immediate development of an asymmetric $2p_{3/2}$ peak characteristic of Cr metal. Figure 2 shows representative C 1*s* EDC's for Cr on C_{60}, together with one obtained after a small amount of C_{60} was deposited on a thick polycrystalline Cr film. For C_{60} adsorbed on Cr, the main line at 284.2 eV was broader with a larger asymmetry than for C_{60} on

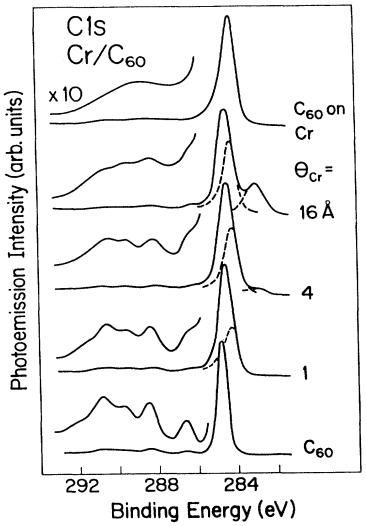

FIG. 2. C 1*s* EDC's for Cr overlayers on C_{60}. Included at the top is the monolayer line shape for C_{60} chemisorbed on Cr, which has a broadened asymmetric main line at 284.2 eV. The dashed lines correspond to the contribution of this feature to the C 1*s* emission. The feature at ~283 eV indicates the formation of Cr-carbide bonding configurations after disruption of fullerenes.

Au, indicative of stronger bonding and, hence, greater electron transfer to the fullerenes.[8] The C 1*s* changes for Cr on C_{60} can be related to interfacial bonding and the dashed lines in Fig. 2 emphasize the contribution from fullerenes in contact with Cr. This interface bonding was readily visible at low coverage, suggesting that the clusters were small and that the surface may be roughened as C_{60} molecules were bonded to the cluster perimeters. After ~12-Å deposition the fullerene surface was covered, since the contribution of the bulk and chemisorbed features decreased at the same rate. For higher coverages the substrate attenuation rate decreased, indicating that the clusters coalesced and produced an irregular metallic layer.

Cr deposition on C_{60} gave rise to a Cr-induced feature in the C 1*s* emission with a binding energy that corresponds to a carbidic bonding configuration. The intensity of this carbidic configuration reached a maximum of ~12 Å when the surface was completely covered and it then decreased at the same rate as the other C 1*s* emission. We associate it with the disruption of surface fullerenes. The intensity of the carbidic feature indicates that between 0.1 and 0.3 fullerene layers were reacted, consuming roughly 1–3 Å Cr. Such a reaction is favorable, albeit weakly, since the heat of formation of Cr carbides in −0.2 eV/atom referenced to the graphitic standard state.[15] In turn, C_{60} is ~0.4 eV/atom less stable than graphite.[16]

At all coverages we observed that the Cr 2*p* core emission had the asymmetry and peak position characteristic of the metallic phase, not the carbide. At higher coverages the Cr 2*p* emission corresponding to the C 1*s* carbidic emission may be buried by the growing metallic clusters. However, its absence at the lowest coverage suggests that Cr cluster growth without disruption occurred initially and that disruption at higher coverages may be mediated by cluster rather than atom reaction. Although energetically favorable, carbide formation from C_{60} may be limited by kinetics or unfavorable bonding geometries. Evidence of this is provided by C_{60} deposition on Cr films, which showed no carbidic emission. This probably results from the minimal distortion of molecular orbitals due to chemisorption on a flat surface, while adsorption on "rough" surfaces may enhance the formation of bonds and lead to disruption, as has been previously suggested.[17] The irregular interface between the clusters and the surface fullerenes may provide such conditions. The dependence on irregular sites would also account for the relatively small amount of the surface disrupted.

The interaction of Cr with C_{60} is also evident from the valence-band spectra shown in Fig. 3. In this case, the photon energy 45 eV was chosen to emphasize the C_{60} features (*p-d* resonant enhancement of the Cr *d* states occurs at higher photon energy[18]). The two leading C_{60} features are π derived while those at higher binding energy have increased σ character.[9,19] Figure 3 shows that the π-derived features broaden more than the σ-derived features upon Cr deposition. This is consistent with results for chemisorbed aromatic molecules when π orbitals are involved in surface bonding.[20] Analysis also shows an apparent reduction in intensity of the π bands relative to the σ bands. Since the equivalent reduction was not observed in spectra acquired at 65-eV photon energy, the effect is probably related to changes in the photoionization cross section associated with chemisorption, and to mixing of fullerene states with Cr *d*-derived states. No spectral features developed in the valence bands that

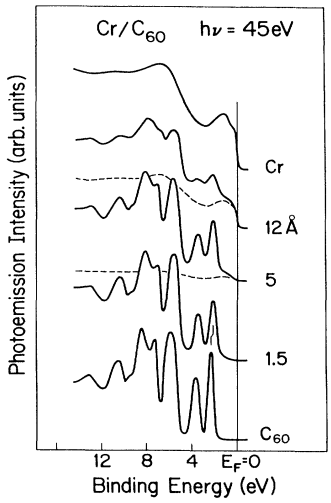

FIG. 3. Valence bands for Cr overlayers on C_{60}. For pure C_{60}, the leading two electronic structures are π derived and the σ character increases at higher binding energy. Cr chemisorption modifies the π components, as shown by the broadening of the first two peaks, and there is a small shift to lower binding energy. Further deposition results in the superposition of C_{60} and Cr metal valence bands.

could be uniquely attributed to new bonding orbitals. Instead, the EDC's appeared to be a superposition of Cr-metal emission (dashed lines, Fig. 3) and broadened fullerene features.

Ti overlayers—Ti-C_{60} bonding and C_{60} disruption

As with the previous overlayers, analysis of the substrate emission shows that Ti atoms did not mix with the fullerene layer. Figure 4 summarizes the valence-band EDC's for Ti deposition onto C_{60}. The deposition of 1.5-Å Ti, corresponding to ~7 Ti atoms per C_{60} surface molecule, shifted the valence-band features 0.5 eV lower in binding energy and produced a new feature at ~0.9 eV below E_F. There was no significant emission at E_F until 6-Å Ti, indicating that Ti-metal species started to form at these higher coverages. We associate the new valence-band feature with a bonding orbital with mixed C $2p$–Ti $3d$ character due to hybridization of LUMO with Ti $3d$ levels. This is the analog of the TiC valence band at ~3.6 eV (Ref. 21) but involves molecular orbitals rather than atomic states and the structure is planar rather than three dimensional. This interpretation is supported by core-level analysis which showed C $1s$ emission consistent with only fullerenes but not carbidic phases and Ti $2p$ emission ~1 eV higher in binding energy than Ti metal. The latter contrasts the low-coverage behavior of Cr, Au, and In core-level emission and demonstrates Ti-C_{60} bonding.

For Ti deposition exceeding ~5 Å, the Ti $2p$ emission evolves toward that of the metal and emission at the Fermi level is increased, indicating the growth of metallic clusters. At this stage, carbidic C $1s$ emission was detected, as in Fig. 2, and its relative intensity reached a maximum at ~12-Å Ti deposition. While the valence-band structures represent superpositions of many bonding configurations, we associate the enhancement of emission at ~3.5 eV with p-d hybrids formed by TiC-like bonding configurations (see EDC at 12 Å). By 40-Å Ti, the valence bands and the Ti $2p$ core levels were dominated by Ti-metal emission since the interface was buried. The development of the Ti $2p$ and valence-band features shows that the initial ~5-Å Ti formed nonmetallic bonds with the surface fullerenes with minimal disruption. At higher coverages Ti nucleates at metallic clusters on this modified surface, and again the equivalent of ~0.2 fullerene layers appear to react to form carbides.

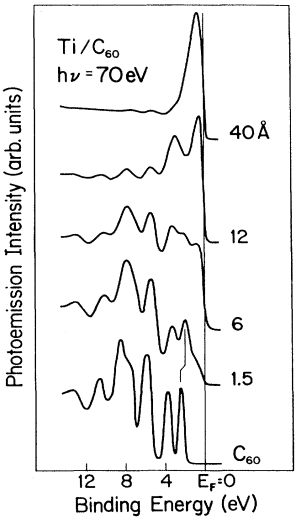

FIG. 4. Valance bands for Ti overlayers on C_{60}. The deposition of less than 1.5 Å of Ti produced a broadening and a shift by 0.5 eV of the C_{60} features. In addition, a new peak formed at 0.9-eV binding energy but there was no emission at the Fermi level. By ~5 Å, a small amount of Ti metal nucleated, as shown by the Fermi-level position on the rising edge of the leading valence-band feature.

La overlayers—La-C_{60} bonding and C_{60} disruption

Studies of the mixing of Ba and Yb with C_{60} have shown the need to deposit at 420 K to produce intermixing in the film.[4,6] For La deposition on C_{60}, however, there was no significant mixing at these temperatures. The C $1s$ EDC's exhibited changes similar to those for Ti and Cr, including coverage of most of the surface after 7 Å and limited carbide formation by 15 Å. The La 3d core-level EDC's for 1-Å deposition demonstrated La-C_{60} bonding with La $3d$ emission that was shifted and broadened relative to the metal. With increased La deposition, the spectra evolved to that of La metal, and intermediate coverage results could be separated into contributions from metallic La clusters and the La-atom-modified surface observed at low coverage. Thus the behavior of La was similar to Ti, with La-C_{60} bonding involving the surface fullerenes followed by La-cluster growth and small amounts of carbide formation at higher coverages.

CONCLUSIONS

In this paper and previous studies we have shown that several processes are in competition during metal-atom adsorption on solid fullerene layers. Clustering (Au, In), limited disruption and carbide formation (Cr, Ti, La), and compound formation (alkali metals, alkaline earth metals, Yb) have all been observed. These processes can be characterized by quantities such as the heat of carbide formation, the bulk metal cohesive energy, the ionization potentials, and the atomic (or ionic) sizes. The absence of La mixing with C_{60} indicates that the large cohesive energy of the bulk metal (4.47 eV/atom) played a dominant role because the ionization energy of La is less than Mg, Yb, and Sr, all of which form fullerides. Moreover, its ionic radius is comparable to fulleride-formers Sr, Ba, K, Rb, and Cs. Metal clustering also occurs for In (cohesive energy 2.52 eV/atom) but not for Ba (cohesive energy 1.9 eV/atom). This establishes a simple guide for determining the dominant processes for vapor deposition onto a fullerene substrate: bulk diffusion and compound formation vs surface diffusion and nucleation.

The results summarized here also demonstrate that fullerenes are susceptible to reaction. Processes that are likely to be cluster mediated result in C_{60} disruption for Ti, Cr, and La, metals that have bulk carbidic phases.

Carbides were not formed for Sr and Yb, even though they have carbidic phases, because fulleride formation is favored. The amount of disruption is estimated to be ~ 0.2 fullerene layers, suggesting a substantial kinetic or coordination barrier at the surface.

Finally, the M-C_{60} bonding tendencies of Ti and La can be understood because La and Ti carbides are characterized by hybridization of metal d and carbon p orbitals. In contrast, Cr-carbide formation involves nonbonding states and the carbide is less stable than the La or Ti carbides.[15,22] This bonding trend is apparent for metals deposited on C_{60}, resulting in surface attachment before cluster growth for Ti and La and subsequent monolayer modification before clustering.

ACKNOWLEDGMENTS

This work was supported by the Office of Naval Research, the National Science Foundation, and the Robert A. Welch Foundation. Stimulating discussions with Y. Z. Li and D. M. Poirier are acknowledged. The synchrotron radiation photoemission experiments were carried out at the NSF-supported Aladdin light source operated by the University of Wisconsin. The assistance of that staff is greatly appreciated.

*Present address: Physics Department, Colorado School of Mines, Golden, CO 80401.

[1]R. C. Haddon *et al.*, Nature **350**, 320 (1991).

[2]A. F. Hebard, M. J. Rosseinsky, R. C. Haddon, D. W. Murphy, S. H. Glarum, T. T. M. Palstra, A. P. Ramirez, and A. R. Kortan, Nature **350**, 600 (1991); K. Holczer, O. Klein, S.-M. Huang, R. B. Kaner, K.-J. Fu, R. L. Whetten, and F. Diederich, Science **252**, 1154 (1991).

[3]P. J. Benning, J. L. Martins, J. H. Weaver, L. P. F. Chibante, and R. E. Smalley, Science **252**, 1417 (1991); P. J. Benning, D. M. Poirier, T. R. Ohno, Y. Chen, M. B. Jost, F. Stepniak, G. H. Kroll, J. H. Weaver, J. Fure, and R. E. Smalley, Phys. Rev. B **45**, 6899 (1992), and extensive references therein to spectroscopic studies.

[4]Y. Chen, F. Stepniak, J. H. Weaver, J. Fure, and R. E. Smalley, Phys. Rev. B **45**, 8845 (1992).

[5]C. Gu, F. Stepniak, D. M. Poirier, M. B. Jost, P. J. Benning, Y. Chen, T. R. Ohno, J. L. Martins, J. H. Weaver, L. P. F. Chibante, and R. E. Smalley, Phys. Rev. B **45**, 6348 (1992).

[6]T. R. Ohno, G. H. Kroll, J. H. Weaver, L. P. F. Chibante, and R. E. Smalley, Phys. Rev. B **46**, 10437 (1992).

[7]R. E. Haufler *et al.*, J. Chem. Phys. **94**, 8634 (1990).

[8]T. R. Ohno, Y. Chen, S. E. Harvey, G. H. Kroll, J. H. Weaver, R. E. Haufler, and R. E. Smalley, Phys. Rev. B **44**, 13747 (1991). See Y. Z. Li, M. Chander, J. C. Patrin, J. H. Weaver, L. P. F. Chibante, and R. E. Smalley, Science **253**, 429 (1991) for results of a scanning tunneling microscope investigation of C_{60} on GaAs (110).

[9]J. H. Weaver, J. L. Martins, T. Komeda, Y. Chen, T. R. Ohno, G. H. Kroll, N. Troullier, R. E. Haufler, and R. E. Smalley, Phys. Rev. Lett. **66**, 1741 (1991).

[10]W. Krätschmer, L. D. Lamb, F. Fostiropoulos, and D. R. Huffman, Nature **347**, 354 (1990); A. F. Hebard, R. C. Haddon, R. M. Fleming, and A. R. Kortan, Appl. Phys. Lett. **59**, 2109 (1991); S. L. Ren, Y. Wang, A. M. Rao, E. McRae, J. M. Holden, T. Hager, K.-A. Wang, W. T. Lee, H. F. Ni, J. Selegue, and P. C. Eklund, *ibid.* **59**, 2678 (1991).

[11]G. Gensterblum, J. J. Pireaux, P. A. Thiry, R. Caudano, J. P. Vigneron, Ph. Lambin, A. A. Lucas, and W. Krätschmer, Phys. Rev. Lett. **67**, 2171 (1991).

[12]H. Ajie *et al.*, J. Chem. Phys. **94**, 8630 (1990).

[13]B. Gumhalter, K. Wandelt, and Ph. Avouris, Phys. Rev. B. **37**, 8048 (1988).

[14]H. Raether, *Excitation of Plasmons and Interband Transitions by Electrons* (Springer-Verlag, Berlin, 1980), p. 51.

[15]*CRC Handbook of Chemistry and Physics,* 69th ed., edited by R. C. Weast (CRC, Boca Raton, FL, 1988), pp. E91 and E92; A. Guillermet and G. Grimvall, Phys. Rev. B **40**, 10582 (1989).

[16]N. Troullier and J. L. Martins, Phys. Rev. B **46**, 1754 (1992); N. Troullier, Ph.D. thesis, University of Minnesota, 1991.

[17]E. Burstein, S. C. Erwin, M. Y. Jiang, and R. P. Messmer, Phys. Scr. (to be published). The authors note that similar behavior is observed with catalytic systems which display chemical reactivity on high index or roughened metal planes but not on low index planes.

[18]J. Barth, F. Gerken, K. L. I. Kobayashi, J. H. Weaver, and B. Sonntag, J. Phys. C **13**, 1369 (1980).

[19]J. L. Martins, N. Troullier, and J. H. Weaver, Chem. Phys. Lett. **180**, 457 (1991).

[20]J. E. Demuth and D. E. Eastman, Phys. Rev. Lett. **32**, 1123 (1974).

[21]L. I. Johansson, A. L. Hagstrom, B. E. Jacobsen, and S. B. M. Hagstrom, J. Electron Spectrosc. Relat. Phenom. **10**, 259 (1977); L. Ramqvist, K. Hamrin, G. Johansson, A. Fahlman, and C. Nording, J. Phys. Chem. Solids **30**, 1835 (1969).

[22]C. D. Gelatt, A. R. Williams, and V. L. Moruzzi, Phys. Rev. B **27**, 2005 (1983).